STOCHASTIC ACTIVE CONTOUR FOR CARDIAC MR IMAGE SEGMENTATION

Charnchai Pluempitiwiriyawej and José M. F. Moura

Electrical and Computer Engineering
Carnegie Mellon University
chanchai@ece.cmu.edu, moura@ece.cmu.edu

Yi-Jen Lin Wu, Shinichi Kanno, and Chien Ho

Pittsburgh NMR Center for Biomedical Research
Carnegie Mellon University

ABSTRACT

We develop an energy based automatic image segmentation algorithm using a novel active contour scheme. The algorithm overcomes some unique challenges arising in cardiac MR images. Two features are particularly relevant. The first is that it uses region-based information captured by a stochastic model. As a result, our method is robust to assumed initial conditions and can be applied to a large range of images, particularly when the contrast is low. The second feature is the incorporation of prior knowledge on the shape of the organ to be segmented. For cardiac image segmentation, it is sufficient to assume that the shape resembles an ellipse.

1. INTRODUCTION

To quantitatively analyze the dynamic function of the heart, it is necessary to segment various parts of the heart chambers in a magnetic resonance (MR) image sequence. In clinical studies, the segmentation task, particularly delineating the epicardium and the left and right ventricular endocardia, is often performed manually, which is time consuming and highly subjective. As a result, the analysis has been limited to only short time sequences per cardiac cycle. To help expedite the process and facilitate the analysis of more comprehensive MR data sets, an automatic and more quantitative approach for analyzing cardiac MR sequence data is desired.

Most of the current active contour methods [1, 2, 3, 4] for medical image segmentation are edge-based, which is very sensitive to noise and initialization. If the initial contour is not close enough to the true boundary of the object, the contour may not evolve or may be trapped at spurious edge points. To overcome these problems, often, a constant external force is added [2, 5]. However, this leads to another difficulty – the leaking of the evolving contour where the edges of the organ's boundary are weaker than the added force, which is often the case in cardiac MR images.

To provide robustness to initial condition without adding a constant external force, we propose an active contour scheme, which we refer to as *stochastic active contour*. The algorithm includes an additional force that accounts for region-based information modeled under a stochastic assumption. Other active contour methods that also utilize the region-based information are [6, 7, 8].

2. STOCHASTIC ACTIVE CONTOUR

Our goal is to segment a homogeneous object (the left or right ventricular cavity of the heart) from the background (the chest wall or other anatomy) in a cardiac MR image. First, we model the image as a sample from a random field. This stochastic model can be applied to a large range of images, particularly when the contrast between distinct regions is difficult to distinguish by human eyes, and other methods may fail. Second, we develop a new active contour scheme that utilizes the *stochastic* region-based information in addition to the edge information of the image. While the region-based information is obtained directly from the original image assuming the stochastic model, the edge information comes from the edge map of the image. The region-based information provides forces on the contour front where the edge information is missing or when the contour front encounters spurious edges. As a result, our method is robust to noise and to the initial condition of the contour. In addition, since our algorithm does not include any constant image-independent force, the problem of contour leakage does not occur. Third, we incorporate the prior knowledge about the shape of the object into the segmentation scheme to overcome the problem with the papillary muscle, which frequently appears in cardiac MR images. Finally, we implement the algorithm using the level set method [9].

Given an image, our goal is to develop a method that automatically finds a contour C that separates the pixels of the image into two groups: the object (the heart) and the background. The method is motivated by the following:

1. Model matching: We assume that the pixel intensity of the object and the background follows different stochastic models: for pixels belonging to the heart, their corresponding intensities are modeled by the stochastic model $\mathcal{M}_1$; for pixels belonging to the background, the corresponding intensity values are described by the stochastic model $\mathcal{M}_2$.
2. Edge information: The contour should capture any nearby salient edges present in the image.
3. Prior knowledge about the shape of the heart: The heart has a nominal contour. We choose to describe it by a generic shape $C_{\mathrm{H}}(\theta)$ parameterized by the parameter vector $\theta = [\theta_1, \ \ldots, \ \theta_n]^T$. The values of these parameters θ_i may determine the detailed size and shape of the object.
4. Smoothness of the contour: The contour of the segmented heart should be smooth, not jagged or too noisy.

We translate these four requirements into an objective functional $J(C)$ with four terms

$$J(C) = \lambda_1 J_1(C) + \lambda_2 J_2(C) + \lambda_3 J_3(C) + \lambda_4 J_4(C), \quad (1)$$

where $J_1(C)$, incorporating the model matching requirement, is called the region-based term; $J_2(C)$ is an edge-based term; $J_3(C)$ incorporates the prior knowledge on the shape of the contour; $J_4(C)$ is the contour smoothing term; and $\lambda_1, \lambda_2, \lambda_3$, and λ_4 are parame-

This work was supported by NIH grants, R01EB/AI-00318 and P41RR-03631, to Pittsburgh NMR Center for Biomedical Research, CMU.

ters that control the relative strength of J_1, J_2, J_3, and J_4, respectively.

Comparing the functional (1) to the classical snake algorithm, the first two terms, $J_1(C)$ and $J_2(C)$, are equivalent to the external energy and the last two terms, $J_3(C)$ and $J_4(C)$, are the internal energy because they control the regularity of the contour. The first and the third terms, $J_1(C)$ and $J_3(C)$, are usually absent in the work reported in the literature.

2.1. Model Matching Term

The goal is to segment the domain Ω of a given image into two "homogeneous" regions separated by the contour C. The region inside the contour, Ω_1, represents the object region. The region outside the contour, Ω_2, corresponds to the background region. A homogeneous region is a region whose intensity is well described by the same statistical model, or equivalently, the same probability distribution. We consider two stochastic models: the model $\mathcal{M}_1$ describes the statistics of the object and the model $\mathcal{M}_2$ represents the statistics of the background. We partition the image pixels $\{(i,j) \in \Omega\}$ into two groups separated by the contour C. If the pixels belong to the object, then the corresponding random variables $\{u_{ij}\}$ should be described by the statistical model $\mathcal{M}_1$. On the other hand, if the pixels belong to the background, the corresponding random variables $\{u_{ij}\}$ are described by the statistical model $\mathcal{M}_2$.

Suppose that the image domain Ω is initially segmented into two regions by a contour C_0, the region inside C_0 called Ω_1 and the region outside C_0 called Ω_2. Let $\mathbf{u}_1(C_0)$ be the vector form of the intensity of the image pixels residing within the contour C_0 and $\mathbf{u}_2(C_0)$ the vector form of the intensity of the image pixels that lie outside C_0.

Given $\mathbf{u}_1(C_0)$ and $\mathbf{u}_2(C_0)$, we update the contour C_0 to maximize the probability that $\mathbf{u}_1$ and $\mathbf{u}_2$ are samples drawn from the object model $\mathcal{M}_1$ and the background model $\mathcal{M}_2$, respectively. To achieve this, we change the contour C_0 to C_1, thereby moving some pixels from Ω_1 to Ω_2 and vice-versa. It is reasonable to control this updating of C_0 to C_1 by attempting to maximize the following functional

$$J_0(C) = \Pr\left\{\{\mathbf{u}_1(C)|\mathcal{M}_1\} \text{ and } \{\mathbf{u}_2(C)|\mathcal{M}_2\}\right\}. \quad (2)$$

Equation (2) represents the probability that all the pixels inside the contour C are generated from the object model $\mathcal{M}_1$ and all the pixels outside the contour C are generated from the background model $\mathcal{M}_2$. If the two events are independent, we have

$$J_0(C) = \Pr\left\{\mathbf{u}_1(C)|\mathcal{M}_1\right\} \cdot \Pr\left\{\mathbf{u}_2(C)|\mathcal{M}_2\right\}. \quad (3)$$

Let p_1 and p_2 be the probability density functions (pdf's) of the models $\mathcal{M}_1$ and $\mathcal{M}_2$, respectively. Then, it can be shown that equation (3) is equivalently rewritten as

$$J_0(C) = p_1(\mathbf{u}_1(C)) \cdot p_2(\mathbf{u}_2(C)). \quad (4)$$

Taking the negative log, equation (4) becomes

$$J_1(C) = -\left[\ln\left(p_1\left(\mathbf{u}_1(C)\right)\right) + \ln\left(p_2\left(\mathbf{u}_2(C)\right)\right)\right], \quad (5)$$

and maximizing $J_0(C)$ in equation (4) becomes minimizing $J_1(C)$ in equation (5).

If we assume further that all pixels $\{u_{ij}\}$ within each region are independent, then

$$p_k\left(\mathbf{u}_i(C)\right) = \prod_{(i,j)\in\Omega_k} p_k\left(u_{ij}\right), \quad k = 1, 2, \quad (6)$$

and equation (5) becomes

$$J_1(C) = -\left[\sum_{(i,j)\in\Omega_1} \ln\left(p_1(u_{ij})\right) + \sum_{(i,j)\in\Omega_2} \ln\left(p_2(u_{ij})\right)\right]. \quad (7)$$

Using level sets [9], C is embedded as the zero level of the level set function ϕ and equation (7) becomes

$$\begin{aligned} J_1(\phi) \;=\; & -\int_\Omega \left[\ln\left(p_1\left(u(x,y)\right)\right)\mathcal{H}_\epsilon(\phi(x,y))\right. \\ & \left. + \ln\left(p_2\left(u(x,y)\right)\right)\left(1-\mathcal{H}_\epsilon(x,y)\right)\right] dxdy, \end{aligned} \quad (8)$$

where

$$\mathcal{H}_\epsilon(\phi) = \frac{1}{2}\left[1 + \frac{2}{\pi}\arctan\left(\frac{\phi}{\epsilon}\right)\right], \quad (9)$$

is the regularized Heaviside function representing the pixels within the contour, and $1 - \mathcal{H}_\epsilon(\phi(x,y))$ is the function representing the pixels outside the contour and the integral is taken over the entire domain Ω of the image. This is the generic form of the main function we want to minimize, and p_1 and p_2 are the assumed pdf's of the object and background models, respectively.

If we assume both the object and the background to be Gaussian with means m_1 and m_2, and variances σ_1^2 and σ_2^2, respectively, then equation (8) becomes

$$\begin{aligned} J_1(\phi) = \int_\Omega \left[\left(\frac{1}{2}\ln(2\pi\sigma_1^2) + \frac{(u(x,y)-m_1)^2}{2\sigma_1^2}\right)\mathcal{H}_\epsilon(\phi(x,y))\right. \\ \left. + \left(\tfrac{1}{2}\ln(2\pi\sigma_2^2) + \tfrac{(u(x,y)-m_2)^2}{2\sigma_2^2}\right)\left(1-\mathcal{H}_\epsilon(\phi(x,y))\right)\right] dxdy. \end{aligned} \quad (10)$$

2.2. Edge-based Term

Our second objective is for the contour to capture the nearby salient edges present in the give image $u(x,y)$. Therefore, we want to minimize

$$J_2(C) = \int_C |\nabla u(C(s))|^2 \, ds, \quad (11)$$

where ∇u is the gradient of the given image $u(x,y)$. Let the regularized delta function,

$$\delta_\epsilon(\phi) = \frac{d}{d\phi}\mathcal{H}_\epsilon(\phi), \quad (12)$$

represents the pixels on the contour C. We can express (11) in terms of the level set function ϕ as

$$J_2(\phi) = \int_\Omega |\nabla u(x,y)|^2 \delta_\epsilon(\phi(x,y)), dxdy. \quad (13)$$

2.3. Prior Knowledge Term

Most current active contour methods [1, 4, 5, 6, 7, 8] only attempt to smooth the curve; they do not impose a particular shape onto the contour. In our application, however, we know that the myocardium part of the heart that we desire to segment resembles an ellipse shape. Therefore, we can exploit this fact and regulate the

shape of the contour not just to be smooth but also to resemble the shape of an ellipse. In this section, we explain how to incorporate the elliptical shape condition into our active contour. We note that the ellipse shape is a crude model. We can possibly use more detailed models for the contour of the myocardium.

An ellipse can be described by a conic equation

$$ax^2 + bxy + cy^2 + dx + ey + f = 0, \tag{14}$$

under the constraint

$$4ac - b^2 > 0. \tag{15}$$

If we collect the ellipse parameters into the vector $\boldsymbol{\theta} = [a \quad b \quad c \quad d \quad e \quad f]^T$ and let the variable vector $\mathbf{v} = [x^2 \quad xy \quad y^2 \quad x \quad y \quad 1]^T$, we can write the ellipse equation compactly as

$$\boldsymbol{\theta}^T \mathbf{v} = 0, \tag{16}$$

under the constraint

$$\boldsymbol{\theta}^T \mathbf{K} \boldsymbol{\theta} > 0, \tag{17}$$

where

$$\mathbf{K} = \begin{bmatrix} 0 & 0 & 2 & 0 & 0 & 0 \\ 0 & -1 & 0 & 0 & 0 & 0 \\ 2 & 0 & 0 & 0 & 0 & 0 \\ 0 & 0 & 0 & 0 & 0 & 0 \\ 0 & 0 & 0 & 0 & 0 & 0 \\ 0 & 0 & 0 & 0 & 0 & 0 \end{bmatrix}. \tag{18}$$

Furthermore, define the ellipse distance function to be

$$\mathcal{D}(x, y) = ax^2 + bxy + cy^2 + dx + ey + f, \tag{19}$$

such that the ellipse constraint (15) holds. This function gives the distance from any arbitrary point (x, y) in the ellipse plane to the ellipse parameterized by $\boldsymbol{\theta}$ [10].

Forcing the shape of the evolving contour C to resemble the ellipse contour $C_H(\boldsymbol{\theta})$,

$$C_H(\boldsymbol{\theta}) = \left\{(x, y) : \boldsymbol{\theta}^T \mathbf{v} = 0 \quad \text{and} \quad \boldsymbol{\theta}^T \mathbf{K} \boldsymbol{\theta} > 0\right\}, \tag{20}$$

is captured by minimizing the squared distance to the ellipse contour $C_H(\boldsymbol{\theta})$ of the pixels on the contour C. In other words, we minimize

$$J_3(C) = \int_C |\mathcal{D}(x, y)|^2 ds. \tag{21}$$

With the level set method, since $\delta_\epsilon(\phi)$ represents the pixels on the contour C, equation (21) becomes

$$J_3(\phi) = \int_\Omega |\mathcal{D}(x, y)|^2 \delta_\epsilon(\phi(x, y)) dx dy. \tag{22}$$

2.4. Contour Smoothing Term

The last desired goal for our method is that the contour of the segmented heart must be smooth, or not too noisy. To achieve this, we minimize the total Euclidean arc length of the contour C [6, 9, 11],

$$J_4(C) = \int_C ds, \tag{23}$$

where ds represents the Euclidean arc length of the contour C. If we minimize $J_4(C)$ alone, the contour C will evolve to become a circle and eventually disappear. However, when we simultaneously minimize $J_4(C)$ along with the other terms in equation (1), the effect of the $J_4(C)$ term will be to force the contour to be smooth. Equation (23) can be rewritten in terms of the level set function as

$$\begin{aligned} J_4(\phi) &= \int_\Omega |\nabla \mathcal{H}_\epsilon(\phi(x, y))| \, dx dy \\ &= \int_\Omega \delta_\epsilon(\phi(x, y)) |\nabla \phi(x, y)| \, dx dy. \end{aligned} \tag{24}$$

3. EVOLUTION OF THE CONTOUR

We evolve the level set function ϕ, thus the contour C, so that it minimizes the functional (1). Applying the Calculus of Variation, the function ϕ that minimizes $J(\phi)$ in equation (1) must satisfy the Euler-Lagrange equation

$$\begin{aligned} 0 = \; & \lambda_1 \left[\frac{1}{2} \ln\left(2\pi\sigma_1^2\right) + \frac{(u - m_1)^2}{2\sigma_1^2}\right] \delta_\epsilon(\phi) \\ & -\lambda_1 \left[\frac{1}{2} \ln\left(2\pi\sigma_2^2\right) + \frac{(u - m_2)^2}{2\sigma_2^2}\right] \delta_\epsilon(\phi) \\ & +\lambda_2 |\nabla u(x, y)|^2 \dot{\delta}_\epsilon(\phi) \\ & +\lambda_3 \cdot |\mathcal{D}(x, y)|^2 \dot{\delta}_\epsilon(\phi(x, y)) \\ & +\lambda_4 \cdot \operatorname{div}\left(\frac{\nabla \phi}{|\nabla \phi|}\right) \delta_\epsilon(\phi), \end{aligned} \tag{25}$$

where $\dot{\delta}_\epsilon(\phi)$ is the derivative of $\delta_\epsilon(\phi)$ with respect to ϕ.

We solve for ϕ in equation (25) by first letting ϕ be a function of time and replace the zero on the left hand side of (25) by the time derivative of ϕ, then iterating it to convergence using the gradient descent method. The algorithm includes an adaptive annealing schedule on the parameter λ_3. Details are omitted due to lack of space.

4. RESULTS

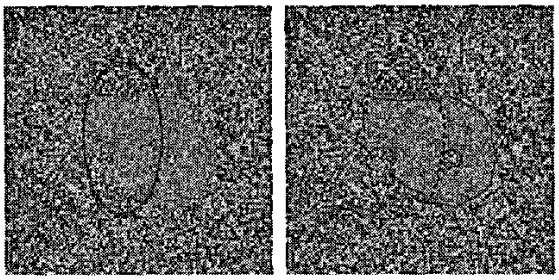

(a) (b)

Fig. 1. Object $\sim \mathcal{N}(0, 4)$, background $\sim \mathcal{N}(0, 25)$.

To demonstrate the effect of the model matching term, we are to segment an image whose object and background are difficult to distinguish by human eyes. such as the one in Fig. 1. The texture of the object, resembling a whistle with a hole in it, is normally distributed with zero mean and variance 4. The background pixels are normally distributed with the same mean but different variance at 25. The initial contour, the dashed line, is an ellipse at the center of the image. The result of the Chan and Vese algorithm [6], as seen in Fig. 1(a), fails to segment the object, i.e., the final contour

stays the same as the initial contour. The result of our stochastic active contour algorithm in Fig. 1(b), however, shows that the final contour converges to the true boundaries of the object.

Fig. 2(a), (b), and (c) show the successful segmentation results of a heart in an MR image using the snake algorithm [4], the Chan and Vese active contour algorithm [6], and our stochastic active contour algorithm, respectively. The initial contours are in dashed lines and the final contours are in solid lines. We can see that the lower part of the contour in the snake algorithm fails to capture the left ventricular endocardium. It evolved out to the edges of the epicardium instead. This is because the edge information at the bottom part of the left ventricular endocardium is too weak. The result in Fig. 2(b) with the Chan and Vese algorithm can delineate the whole boundary of the left ventricular endocardium, but fails to separate the papillary muscles out of the left ventricle, as desired. The result when applying our stochastic active contour algorithm in Fig. 2(c), however, solves the papillary muscle problem and correctly segments both cavities and the heart from the chest wall because we impose the condition about the shape of the contours to resemble an ellipse.

5. REFERENCES

[1] M. Kass, A. Witkin, and D. Terzopoulos, "Snakes: Active contour models," *Internatinal Journal of Computer Vision*, vol. 1, no. 4, pp. 321–331, 1988.

[2] R. Malladi, J. A. Sethian, and B. Vemuri, "Shape modeling with front propagation: A level set approach," *IEEE Transactions on Pattern Analysis and Machine Intelligence*, vol. 17, no. 2, pp. 158–175, February 1995.

[3] V. Caselles, R. Kimmel, and G Sapiro, "Geodesic active contours," in *Proceedings of the 5th Internatinal Conference on Computer Vision (ICCV-95)*, 1995, pp. 694–699.

[4] C. Xu and J. L. Prince, "Snakes, shapes, and gradient vector flow," *IEEE Transactions on Medical Imaging*, vol. 7, pp. 359–369, March 1998.

[5] L. D. Cohen, "On active contour models and balloons," *CVGIP: Image Understanding*, vol. 53, no. 2, pp. 211–218, March 1991.

[6] T. F. Chan and L. A. Vese, "Active contours without edges," *IEEE Transactions on Image Processing*, vol. 10, no. 2, pp. 266–277, Febuary 2001.

[7] A. Chakraborty, L. H.Staib, and J. S. Duncan, "Deformable boundary finding in medical images by integrating gradient and region information," *IEEE Transactions on Medical Imaging*, vol. 15, no. 6, pp. 859–870, December 1996.

[8] A. Yezzi Jr., A. Tsai, and A. Willsky, "A statistical approach to snakes for bimodal and trimodal imagery," in *The Proceedings of the Seventh IEEE International Conference on Computer Vision*, 1999, vol. 2, pp. 898 –903.

[9] J. A. Sethian, *Level Set Methods and Fast Marching Methods*, Cambridge University Press, 1999.

[10] Andrew W. Fitzgibbon, Maurizio Pilu, and Robert B. Fisher, "Direct least square fitting of ellipses," *IEEE Transactions on Pattern Analysis and Machine Intelligence*, vol. 21, no. 5, pp. 476–480, 1999.

[11] Guillermo Sapiro, *Geometric Partial Differential Equations and Image Analysis*, Cambridge University Press, 2001.

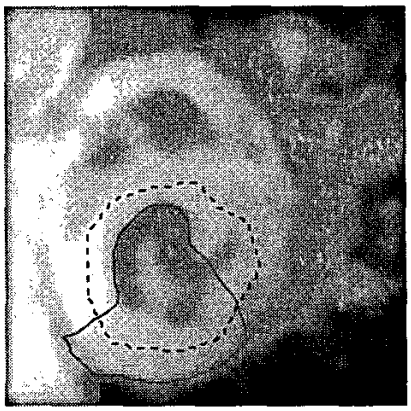

(a) Snake algorithm.

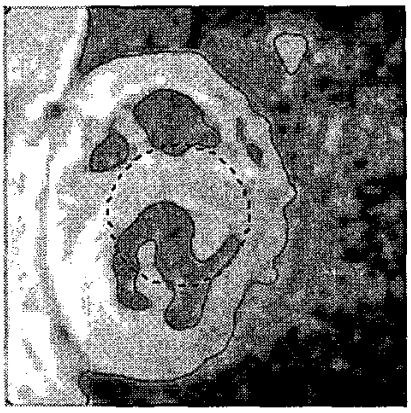

(b) Chan and Vese active contour algorithm

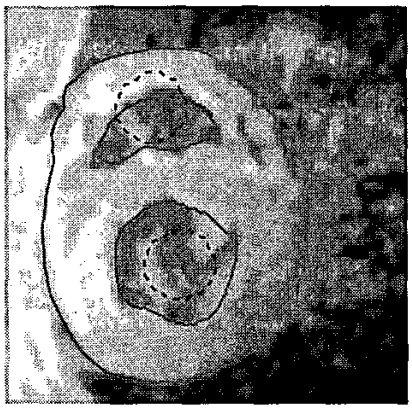

(c) Stochatic active contour algorithm

Fig. 2. Segmentation results of a cardiac MR image using different algorithms.